Plasticity of HP1 proteins in mammalian cells

George K. Dialynas[1], Stefan Terjung[2], Jeremy P. Brown[3], Rebecca L. Aucott[4], Bettina Baron-Luhr[5], Prim B. Singh[5] and Spyros D. Georgatos[1,*]

[1]The Stem Cell and Chromatin Group, Laboratory of Biology, The University of Ioannina, School of Medicine and The Institute of Biomedical Research (FORTH/BRI), 45 110 Ioannina, Greece
[2]Advanced Light Microscopy Facility (ALMF), European Molecular Biology Laboratory, D-69117 Heidelberg, Germany
[3]Children's Hospital Oakland Research Institute, 5700 Martin Luther King Jr Way, Oakland, CA 94609, USA
[4]Tissue Fibrosis and Remodelling Group MRC/University of Edinburgh Centre for Inflammation Research, The Queen's Medical Research Institute, 47 Little France Crescent, Edinburgh, EH16 4TJ, UK
[5]The Division of Tumor Biology, Department of Immunology and Cell Biology, Forschungszentrum Borstel, D-23845 Borstel, Germany
*Author for correspondence (e-mail: sgeorgat@cc.uoi.gr)

Accepted 18 July 2007
Journal of Cell Science 120, 3415-3424 Published by The Company of Biologists 2007
doi:10.1242/jcs.012914

Summary

We have compared the distribution of endogenous heterochromatin protein 1 (HP1) proteins (α, β and γ) in different epithelial lines, pluripotent stem cells and embryonic fibroblasts. In parallel, we have interrogated assembly and dynamics of newly expressed HP1-GFP proteins in cells lacking both HP1α and HP1β alleles, blocked at the G1-S boundary, or cultured in the presence of HDAC and HAT inhibitors. The results reveal a range of cell type and differentiation state-specific patterns that do not correlate with 'fast' or 'slow' subunit exchange in heterochromatin. Furthermore, our observations show that targeting of HP1γ to heterochromatic sites depends on HP1α and H1β and that, on an architectural level, HP1α is the most polymorphic variant of the HP1 family. These data provide evidence for HP1 plasticity under shifting microenvironmental conditions and offer a new conceptual framework for understanding chromatin dynamics at the molecular level.

Key words: HP1, Chromatin, Stem cells

Introduction

Heterochromatin protein 1 (HP1) proteins are conserved constituents of nearly all eukaryotic cells (Singh et al., 1991). These proteins possess a characteristic, modular architecture and consist of three structural domains: an amino-terminal chromodomain (CD), a flexible 'hinge' region and a carboxyl-terminal chromo-shadow domain (CSD) that is structurally related to the CD. Because of this quasi-symmetric structure, it is believed that HP1 proteins have arisen by duplication of a single ancestral gene encoding the CD (Brasher et al., 2000; Cowieson et al., 2000) (reviewed by Singh and Georgatos, 2002).

In mammals there are three HP1 variants, α, β and γ (reviewed by Jones et al., 2000). These proteins have a propensity to homo- or heterodimerize, associate with chromatin through histone H3 (trimethylated at lysine 9, or unmodified) and serve either as gene repressors or as gene activators (see de Wit et al., 2007) (reviewed by Eissenberg and Elgin, 2000; Hediger and Gasser, 2006). However, despite the obvious structural and biochemical similarities, HP1 variants appear to have non-redundant functions (Filesi et al., 2002; Schott et al., 2006; Cammas et al., 2007) and distinct localization. In cultured cells, HP1α and HP1β are found predominantly in foci of constitutive heterochromatin, whereas HP1γ shows an indistinct, 'pan-nuclear' distribution (Bartova et al., 2007; Horsley et al., 1996; Minc et al., 1999; Nielsen et al., 1999; Schott et al., 2006; Smothers and Henikoff, 2001). To date, the factors that determine the 'regional' specificity and the functional specialization of these structurally similar proteins remain unknown.

FRAP (fluorescence recovery after photobleaching) analysis provides interesting clues as to how HP1 proteins may behave in different nuclear mileux. Thus, in euchromatin, the binding of HP1 proteins seems to be transient and the entire pool turns over in about 5 seconds (Cheutin et al., 2003). A transiently associating pool is also found in heterochromatin, with a residence time of around 60 seconds, although a small fraction (approximately 1-5%) that might 'seed' the formation of higher order complexes is relatively immobile (Dialynas et al., 2006; Festenstein et al., 2003; Schmiedeberg et al., 2004). There are indications that HP1 dynamics are modulated during cellular differentiation or entry into a growth-arrest state (Cheutin et al., 2003; Festenstein et al., 2003; Meshorer et al., 2006). However, it is still unclear to what extent the steady-state distribution and the accumulation of HP1 proteins in distinct territories is solely determined by binding to methylated lysine 9 on histone H3 (me_3K9-H3) (Bannister et al., 2001; Jacobs and Khorasanizadeh, 2002; Lachner et al., 2001), or requires auxiliary factors (Eskeland et al., 2007), an RNA component (Maison et al., 2002) and HP1-specific modifications (Lomberk et al., 2006).

Prompted by current controversies, we have compared the localization of HP1 variants in different cellular models and examined HP1 assembly, in mammalian cells that were metabolically challenged or genetically manipulated. The results reveal alternative distribution patterns and distinct specificities with regards to chromatin targeting that do not conform to the current dogma of a me_3K9-H3-anchored protein network. Instead, the data show that localization of the three HP1 variants to different chromatin territories exhibits plasticity and depends on cellular context, cell cycle signals and developmental cues. The new information better describes HP1micro-states and unifies a variety of previous observations.

Results

HP1 proteins form variant-specific assemblies

To compare the sub-nuclear distribution of HP1 proteins we systematically screened different mammalian cell lines by confocal microscopy (for details see Materials and Methods). Consistent with previous studies, staining of human (HeLa) and mouse (C127) cells with anti-HP1γ antibodies yielded a diffuse, pan-nuclear pattern, suggesting that this protein is evenly distributed among heterochromatic and euchromatic territories (GFP 1A, HP1γ). By contrast, staining with anti-HP1α and anti-HP1β antibodies yielded a range of 'speckled' patterns superimposed on diffuse fluorescence, indicating preferential (yet, not exclusive) association with heterochromatic domains (Fig. 1A, HP1α/HP1β).

Surprisingly, although HP1α and HP1β accumulated in heterochromatic regions, they did not completely overlap with each other and were not exactly coincident with me_3K9-H3 sites (Fig. 1B,C). Furthermore, we noticed that heterochromatic accumulations of HP1α often had irregular borders and could be resolved into a constellation of smaller clusters, whereas HP1β 'blocks' were always compact and had an ovoid shape (Fig. 1D). Assessment of the relative fluorescence intensity/unit area revealed quantitative differences in the abundance of HP1α and HP1β between HeLa and C127 cells, as shown in Fig. 1E. In addition, the number of HP1α and HP1β foci per cell varied, consistent with distinct distribution modes (Fig. 1F). With minor variations, the same results were obtained when human MCF-7, HEMEC, AS49, SW480 and SKOV3 cells, mouse 3T3 cells, rat NRK cells and dog MDCK-II cells were examined (data not shown), suggesting that, despite the overlap, each HP1 protein forms distinct assemblies.

To explore further the in situ organization and intrinsic properties of each HP1 variant, we permeabilized cultured cells (C127) with Triton X-100 and washed out all soluble components. Western blotting indicated that a significant proportion of endogenous HP1α, HP1β and HP1γ is released upon detergent extraction (Fig. 2A, compare lanes W, Pt and S1). An additional fraction of HP1 proteins (in most cases HP1α) was also removed from the nucleus after subsequent digestion with RNAse A (Fig. 2A, lanes S2), but the amount of the material released in the supernatant varied from experiment to experiment.

To find out whether the 'heterochromatic' and 'euchromatic' pools of the three HP1 proteins were differentially affected by

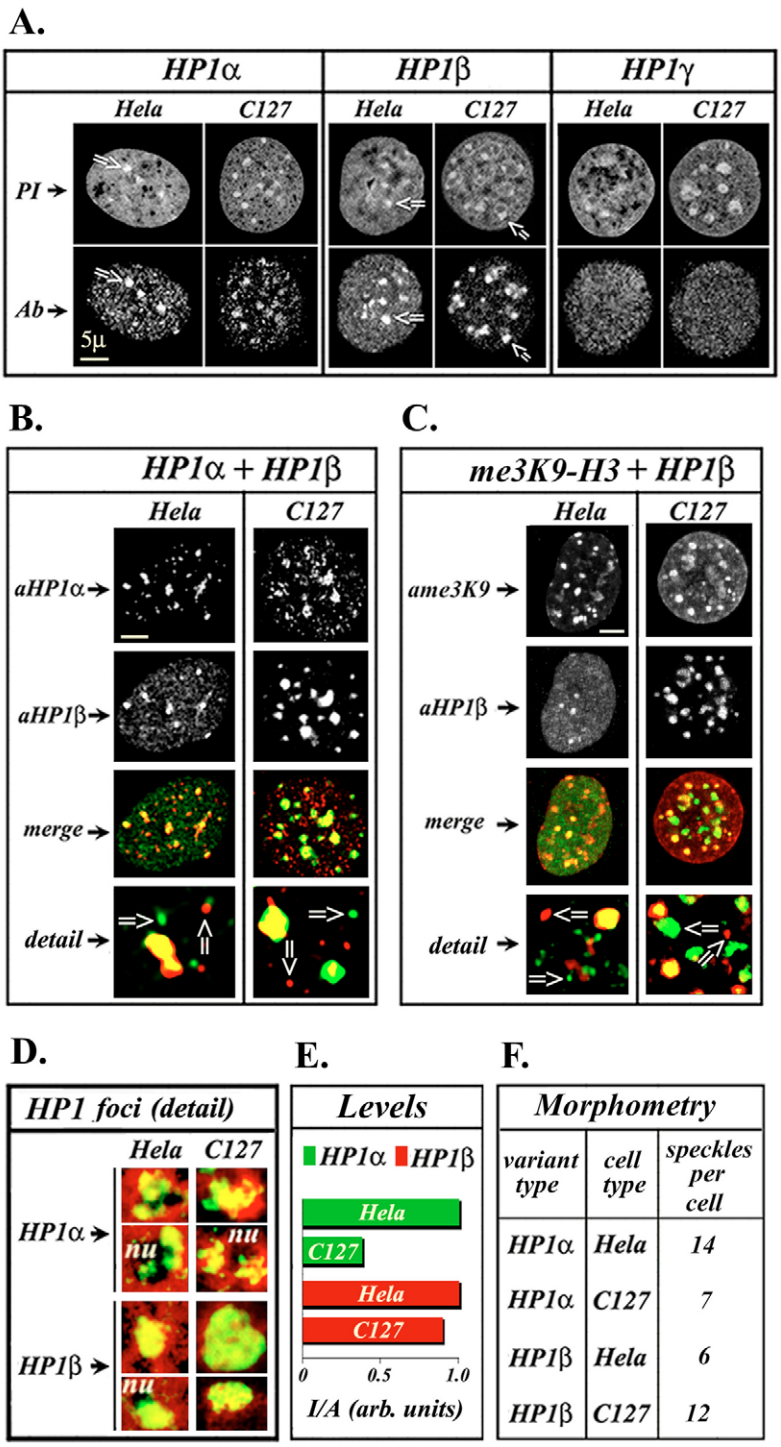

Fig. 1. Distribution of endogenous HP1 proteins in human and mouse cell lines. (A) Staining of HeLa and C127 cells with antibodies (Ab) to HP1α, HP1β and HP1γ. Propidium iodide (PI) staining of the cells is also shown. Arrows indicate major heterochromatic foci. (B) Double staining of the same cells with anti-HP1α (red) and anti-HP1β (green) antibodies. (C) Double immunofluorescence as in B using anti-HP1β (green) and anti-me_3K9-H3 (red) antibodies. Arrows in the enlarged images indicate lack of colocalization. (D) Detail of HP1α and HP1β foci (green) counter-stained with PI (red) at high contrast and higher magnification. nu, nucleolus. (E) Relative fluorescence intensity per unit of nuclear surface (I/A; in arbitrary units) in antibody-stained cells. (F) Average number of HP1α and HP1β foci (3 μm or greater in diameter) in HeLa and C127 cells as detected after morphometric analysis. Successive optical sections and 'projections' from 15 cells were analyzed in each case. Bars, 5 μm. Note: In this and all subsequent figures, merged images are displayed in color, whereas individual red and green profiles are reproduced in grayscale to minimize differences in the visual perception of the red and green color.

these treatments, we stained the Triton-ghosts before and after RNase digestion with anti-HP1 antibodies. As shown in Fig. 2C-E (+TX panels), most of the HP1γ protein was removed by the detergent, except for a small amount of material that remained bound to heterochromatic foci. In contrast to this, the overall pattern of HP1α and HP1β in Triton-ghosts was very similar to that of non-extracted cells (compare Fig. 2C-E with Fig. 1A), suggesting that the major part of these proteins is strongly associated with heterochromatin. When Triton-ghosts were digested with RNase, no further changes were observed (Fig. 2C-E, +TX/RNase). This was not due to inefficient RNA digestion, because the same treatment resulted in the complete loss of B23, a nucleolar protein that binds RNA [Fig. 2B; for more information see Pinol-Roma (Pinol-Roma, 1999) and Zatsepina et al. (Zatsepina et al., 1997)].

When Triton-ghosts were incubated with low concentrations of purified, GST-fused HP1α or HP1β, we could detect robust binding to all heterochromatic regions (Fig. 2F, +HP1α-GST/HP1β-GST, TX rows). However, this was not seen when the specimens were incubated with the same concentrations of recombinant HP1γ (Fig. 2F, +HP1γ-GST, TX rows), suggesting either a lack of direct interactions or that heterochromatic sites were fully 'saturated' with endogenous HP1γ (for additional information see below). Finally, when Triton-ghosts were treated with RNase A before incubation with recombinant proteins, binding of HP1α-GST and HP1β-GST was not significantly affected (Fig. 2F, TX/RNase rows). Taken together, these data suggest that the three HP1 variants are differently organized and that 'bulk' RNA does not contribute significantly to HP1-heterochromatin interactions.

HP1 proteins are dynamically and differentially distributed in ES cells

We next wanted to investigate whether the spatial distribution of HP1 variants depends on differentiation state. To this end, we examined mouse embryonic stem (ES) cells (E14) (see Nichols et al., 1990) cultured in the presence or absence of leukemia inhibitory factor (LIF). As shown in Fig. 3A, there was obvious heterogeneity in the subnuclear organization of HP1α and HP1γ in undifferentiated ES cells. In other words, although some of the cells possessed sizable heterochromatic

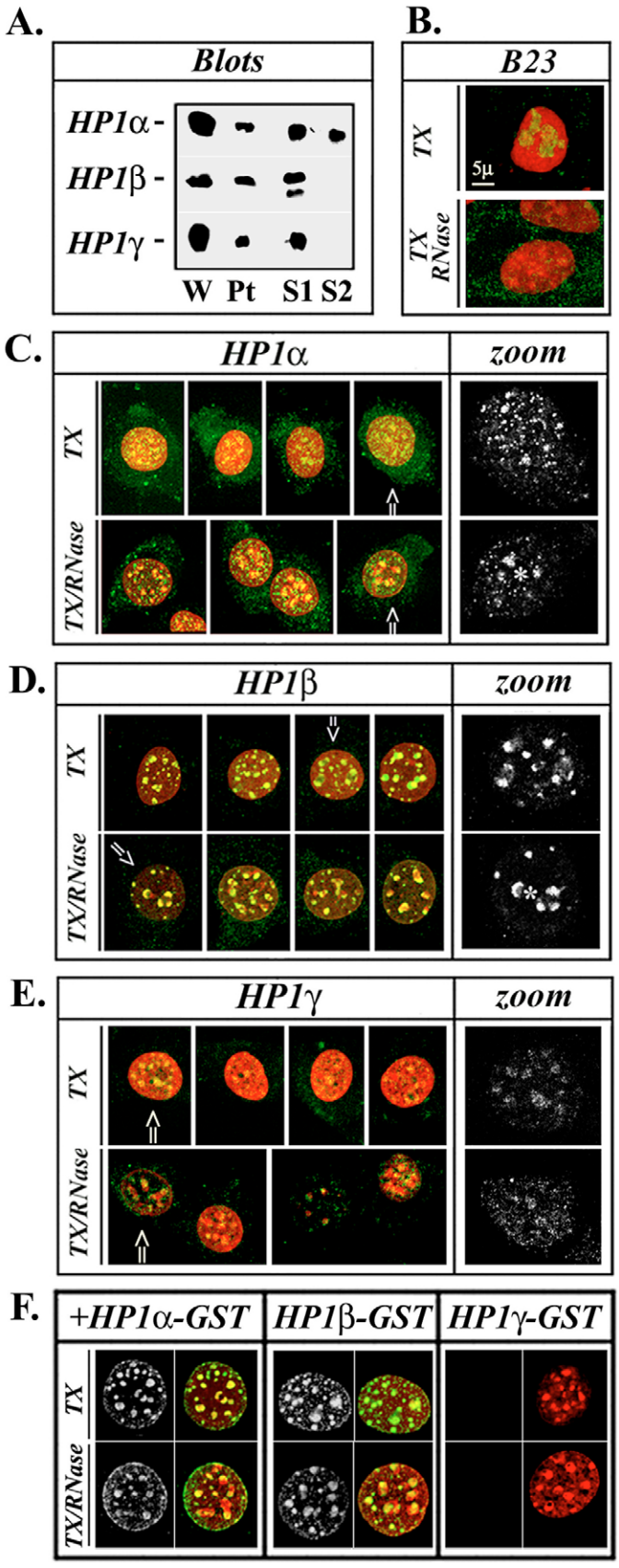

Fig. 2. Differential stability of HP1 assemblies to detergent extraction and RNase digestion. (A) Partitioning of HP1 proteins after permeabilization with Triton X-100 and subsequent treatment with RNase A, as assessed by western blotting. Lanes: W, whole cell lysate; Pt, insoluble residue; S1, material released by Triton; S2, material released by the subsequent RNase digestion.
(B) Distribution of the nucleolar protein B23 (control) after treatment with Triton alone or Triton followed by RNase. Note that the protein is not removed from the nucleoli by the detergent alone, but is fully removed after a combined Triton and RNAse treatment. Only merged images are shown (green: antibody staining; red: PI).
(C-E) Distribution of HP1 proteins under conditions similar to those described in (B). A gallery of merged images in 'projection' mode are shown on the left (green: antibody staining; red: PI), and selected and highly magnified sections are depicted on the right. Arrows indicate the cells from which these sections were taken and asterisks denote the position of nucleoli. (F) In situ binding of recombinant HP1 proteins (0.25 μg/ml) to Triton-ghosts and Triton/RNase A-ghosts. For each protein, antibody staining (anti-GST) is presented on the left, and the merged image after counter-staining with PI is depicted on the right. The profiles are of C127 cells. Analogous experiments with HeLa cells yield similar results. Bar, 5 μm.

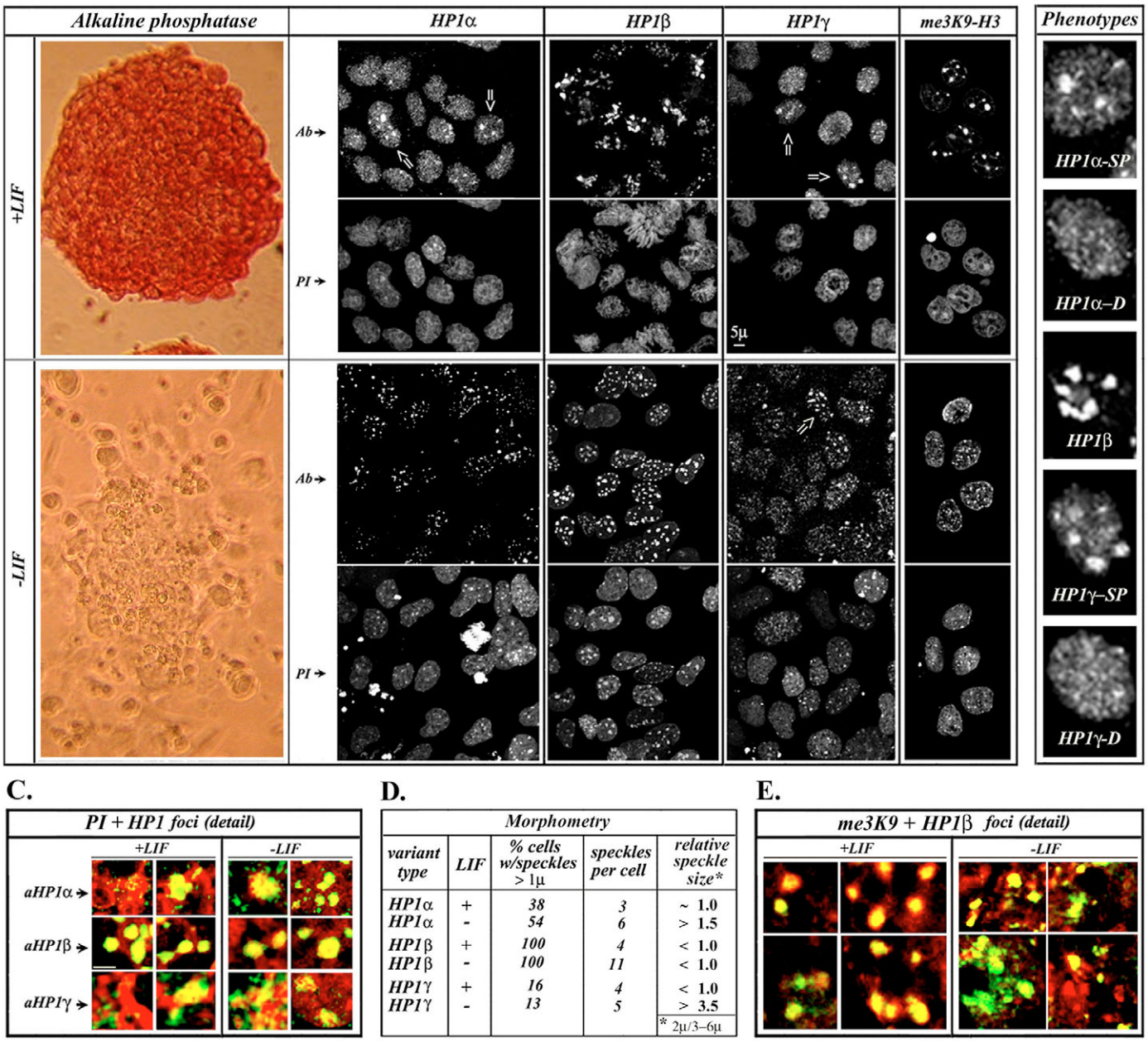

Fig. 3. Distribution of HP1α, HP1β, HP1γ and me_3K9-H3 in mouse ES cells. (A) The colored panels on the left show alkaline phosphatase staining, while the gallery on right depicts propidium iodide (PI) and antibody stained (Ab) E14 cells maintained in the presence (+) or absence (–) of LIF. Arrows indicate cells with a speckled pattern. (B) Some of the cells depicted in A magnified 3×. SP, speckled pattern; D, diffuse, 'micrograniular' pattern. (C) High contrast and high magnification images of HP1α, HP1β and HP1γ foci (green) counter-stained with PI (red). (D) Morphometric data depicting the proportion of cells exhibiting a speckled phenotype, the average number of foci per cell and the relative size of foci (ratio of particles measuring 2 μm to particles measuring 3-6 μm) in each sample. The data represent averages from at least 50, optically sectioned cells. (E) High contrast and high magnification images of double staining of undifferentiated and differentiated E14 cells with antibodies to HP1β (green) and me_3K9-H3 (red). Bars, 5 μm.

'spots', neighboring figures often exhibited a rather diffuse, 'micrograniular' pattern. This was not due to cellular damage and heterochromatin disorganization, because a diffuse distribution pattern was never observed with HP1β (compare the corresponding profiles shown in Fig. 3A +LIF; for more details see Fig. 3B,C).

Morphometric analysis (Fig. 3D) confirmed our visual impression, demonstrating that the majority of the undifferentiated cells had a diffuse HP1α phenotype, with the typical speckled pattern restricted to only 38% of all figures. A similar 'divide' was detected in the distribution of HP1γ, with a significant proportion of cells possessing large heterochromatic foci and the rest exhibiting the usual diffuse fluorescence pattern previously observed in HeLa and C127

cells. Of note here is the fact that the cells exhibiting a speckled or a diffuse pattern were dispersed within each colony and did not form clusters or 'zones'.

When LIF was removed from the medium and ES cells were allowed to differentiate, the HP1 patterns changed in subtle, yet morphologically distinguishable, ways (Fig. 3A,C –LIF; for morphometric data see Fig. 3D). Consistent with results reported recently by Meshorer and co-workers (Meshorer et al., 2006), the average number of HP1α foci per cell doubled, whereas individual foci were smaller. An even greater increase in the number of foci per cell was observed for HP1β, without a significant change in the size of the particles. Finally, HP1γ followed a third re-distribution pattern, with the number of foci per cell increasing only slightly, but the sizes of particles becoming significantly smaller.

The heterogeneity of HP1α and HP1γ patterns suggested the existence of different chromatin 'states' or epigenetic 'regimes', even within the same colony of ES cells. Furthermore, the data showed that HP1γ could accumulate in heterochromatic sites, similarly to HP1β and HP1α, under certain developmental conditions. To assess whether these dynamic changes were paralleled by changes in heterochromatin structure, we stained the cells with antibodies recognizing me_3K9-H3. Although heterochromatic foci possessing this marker were always smaller in differentiated cells than in undifferentiated cells (following the trend of HP1α and HP1γ), there was not any significant cell-to-cell variability in the distribution of me_3K9-H3 (Fig. 3A, compare panels me3K9 in +LIF and –LIF samples) and the patterns generally resembled those of HP1β (Fig. 3E). The fact that the patterns of me_3K9-H3 and of HP1β were invariable at each step of in vitro differentiation, whereas those of HP1α and HP1γ were highly polymorphic, strongly suggests the existence of distinct epigenetic states even among cells that are phenotypically similar and have a clonal origin (for further comments see the Discussion).

Distinct targeting modes of transfected HP1 proteins in human and mouse cells

We have shown previously that transient expression of HP1β-GFP in human cells (HeLa and MCF-7) yields two different phenotypes: in a subset of cells the fluorescent protein rapidly accumulates at heterochromatic sites (SP phenotype), whereas in another group of cells HP1β-GFP is largely dispersed (D phenotype). The two distribution modes are not dependent on expression level, but the D pattern is gradually converted to a SP pattern, as cells progress through S phase. This does not occur upon G1-S arrest (Dialynas et al., 2006).

Extending these observations, we expressed HP1α-GFP, HP1β-GFP and HP1γ-GFP in cells of different origin and compared their spatial distribution 7-12 hours after transfection. As shown in Fig. 4A, transient expression of HP1α-GFP and HP1β-GFP in HeLa cells resulted in both the SP and the D phenotypes, whereas expression of HP1γ-GFP resulted in only the D phenotype. This was never seen in C127 cells, in which only SP patterns were observed, even with HP1γ-GFP, suggesting that the different cell types may 'handle' differently the newly synthesized HP1 proteins.

Similarly to endogenous HP1α/β, HP1α/β-GFP extensively overlapped, but did not exactly colocalize, with me_3K9-H3 sites (Fig. 4B). Furthermore, assessment of the relative fluorescence levels per unit of nuclear surface in cells exhibiting a SP or a D phenotype (Fig. 4C) did not reveal significant differences, reinforcing our previous conclusion that the localization patterns do not correlate directly with expression levels [for relevant data see also Dialynas et al. (Dialynas et al., 2006)].

That the newly synthesized HP1-GFP proteins follow different fates in human and mouse cells could be convincingly demonstrated using two HP1β deletion mutants, one containing and one lacking the CD. As shown in Fig. 4D, both mutants gave a D phenotype in HeLa cells. However, CD-GFP was recruited quantitatively to heterochromatic sites in C127 cells. This effect was specific, because the other mutant (ΔCD-GFP), which lacks a histone H3-binding site, was unable to assemble at heterochromatic regions and remained diffuse in mouse cells. The patterns observed in C127 cells did not represent an exceptional case and could be reproduced in all mouse lines tested (e.g. 3T3 and mouse embryonic fibroblasts; see below), consistent with a genuine species-specificity.

To confirm these results by a different approach, we exploited our earlier observations (Dialynas et al., 2006) and examined the fate of HP1-GFP proteins in transfected cells blocked at the G1-S boundary with hydroxyurea. As shown in Fig. 4E, upon transfection with the corresponding plasmids, human cells exhibited a D phenotype, whereas C127 cells exhibited an SP phenotype, indistinguishable from that of the non-arrested cells. We were able to rule out the trivial possibility that C127 cells were refractory to S phase blockers and further substantiate these results by repeating the drug treatment and monitoring BrdU and Cy3dUTP incorporation (data not shown).

Since the targeting of HP1-GFP proteins to heterochromatin appeared to be dependent on cellular context, we found it crucial to compare their intracellular dynamics in human and mouse cells. Quantitative data presented in Fig. 4F reveal that heterochromatin-bound HP1α-GFP and HP1β-GFP exhibited similar dynamics in HeLa and C127 cells, whereas heterochromatin-associated (C127 cells) or diffusely distributed (HeLa cells) HP1γ was noticeably more mobile than these two variants. From these experiments we conclude that, although HP1-GFP proteins follow different fates and utilize different mechanisms to target heterochromatin in human and mouse cells, their main properties are almost the same.

Consistent with this interpretation, the 'immobile' fraction of the three HP1-GFP proteins, as assessed by the percentage fluorescence recovery at plateau, ranged between 2.5 and 5.3%, indicating that the proportion of tightly-bound HP1 was, in all cases, quantitatively minor (see also Dialynas et al., 2006). That this minor fraction represented a slowly exchanging sub-population of HP1 molecules and not photodamaged material could be proved by repeating the FRAP experiments with GFP alone (Fig. 4F, gfp), or assessing HP1 dynamics after treatment of the cells with sodium butyrate (see below).

Prompted by these findings, we further examined the mouse system trying to define conditions under which the incorporation of HP1-GFP proteins into heterochromatic foci is aborted. For these purposes, we treated C127 cells with the HDAC inhibitors sodium butyrate and trichostatin A (TSA) or, alternatively, with the p300/CBP HAT inhibitor curcumin. As

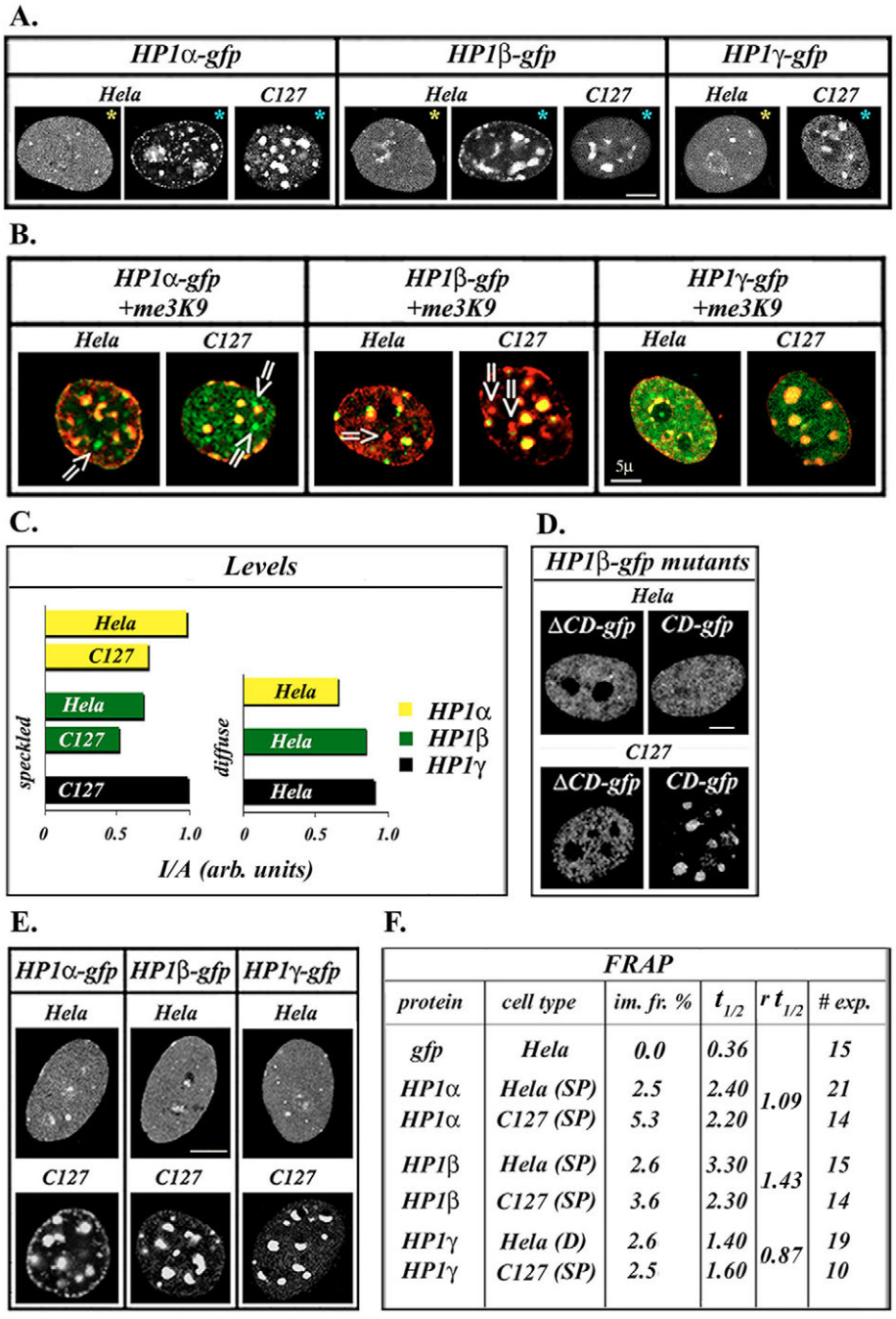

Fig. 4. Fate and dynamics of newly expressed HP1-GFP proteins in human and mouse cell lines. (A) Distribution of HP1-GFP proteins expressed in HeLa and C127 cells. Representative examples of the 'diffuse' (D, white asterisks) and the 'speckled' (SP, blue asterisks) phenotypes are shown. (B) Relative distribution of HP1-GFP and me_3K9-histone H3 (as detected by a specific antibody) in the two cell types. Only merged images are shown (HP1-GFP: green, me_3K9-H3: red). Arrows indicate sites where the two markers do not coincide. (C) Relative fluorescence intensity per unit of nuclear surface (I/A; in arbitrary units) in samples of transfected cells. Successive optical sections and 'projections' from at least 15 cells were analyzed in each case. (D) Profiles of HeLa and C127 cells transfected with a chromodomain containing (CD-GFP) and a chromodomain-lacking (ΔCD-GFP) mutant of HP1β. Observe that CD-GFP assembles correctly in mouse cells, but remains diffuse in human cells. (E) Distribution of HP1-GFP proteins in the same cell lines used in (A) after S phase block with hydroxyurea. Note that HP1α/HP1β are diffuse in human cells, but continue to form large foci in mouse C127 cells. Also notice that the targeting of HP1γ-GFP in the mouse system is not affected by S phase blocking. (F) FRAP data from transfected HeLa and C127 cells. Fluorescence recovery half-times ($t_{1/2}$) are in seconds. $rt_{1/2}$ is the ratio of the half-times in the two cell types; im. fr. is the immobile fraction. Bars, 5 μm.

seen in Fig. 5A, curcumin did not have any effect on the localization of HP1α and HP1β-GFP, whereas TSA and sodium butyrate had a selective effect, with roughly 30% of the interphase cells presenting the D phenotype [for relevant data see also Bartova et al. (Bartova et al., 2005)]. Interestingly, whereas the localization patterns of the two proteins in butyrate-treated cells were markedly different from those of non-treated controls, the fluorescence recovery half-times of HP1α-GFP and HP1β-GFP were only slightly altered (less than 50%) upon treatment with HDAC inhibitors (Fig. 5B). However, no measurable immobile fraction of HP1α-GFP and HP1β-GFP could be detected in the span of these experiments, consistent with the fact that histone hyperacetylation has a profound, destabilizing effect on HP1.

Heterochromatic localization of HP1γ is dependent on HP1α and HP1β

It has been shown that HP1 proteins are able to homo- and heterodimerize through interactions that involve the CSD (Brasher et al., 2000). We reasoned that if this were true in vivo, variation in HP1 distribution may arise from 'trans-dominant' effects, i.e. a 'heterochromatic' variant may target a 'euchromatic' variant to pericentromeric heterochromatin (and the other way around) under certain conditions. Focusing on this problem, we studied the fate and distribution of the three HP1 proteins in mouse embryonic fibroblasts (MEFs) in which all HP1α and HP1β alleles had been disrupted (details on the knockouts will be published elsewhere).

Data depicted in Fig. 6A,B confirm that endogenous HP1α and HP1β were completely absent in double-null cells. As expected, staining of wild-type MEFs with anti-HP1β antibodies yielded a clearly heterochromatic pattern, whereas staining with anti-HP1γ antibodies gave a diffuse pattern in all cells (Fig. 6A, HP1β and HP1γ). However, the distribution of HP1α was heterogeneous, as previously observed in

A.

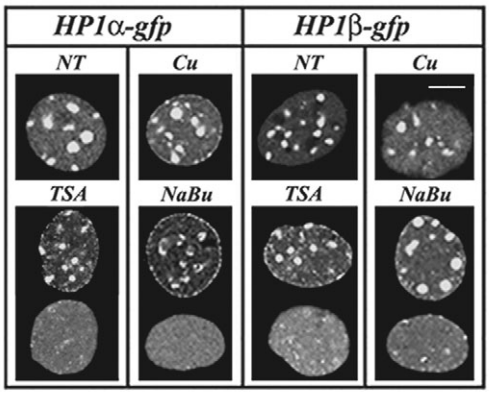

B.

FRAP				
protein	*cell type*	*im. fr. %*	$t_{1/2}$	*# exp.*
HP1α	Hela (D)	0.0	2.0	16
HP1α	C127 (D)	0.0	2.2	21
HP1β	Hela (D)	0.0	1.7	15
HP1β	C127 (D)	0.0	1.5	22

Fig. 5. Effect of HAT and HDAC inhibitors on HP1 localization. (A) Distribution of HP1α-GFP and HP1β-GFP in C127 cells treated with buffer (NT), curcumin (Cu), Trichostatin A (TSA) and sodium butyrate (NaBu). Note that HDAC inhibitors cause randomization of HP1 proteins in a subset (~30%) of cells. The same results are obtained with HeLa cells (not shown). (B) FRAP data from cells treated with NaBu and exhibiting the diffuse (D) phenotype. Fluorescence recovery half-times ($t_{1/2}$) are in seconds; im. fr. is the immobile fraction. Note that the immobile fraction disappears and the fluorescence recovery half-times become shorter in comparison to those of non-treated cells (see Fig. 4F). Bar, 5 μm.

undifferentiated ES cells, yielding either a 'dispersed' or a 'speckled' phenotype (Fig. 6A, HP1α, compare with Fig. 3A). The pattern of me_3K9-H3 did not differ in wild-type and mutant cells (Fig. 6A, me3K9), indicating that heterochromatic territories are not affected by the absence of HP1α and HP1β.

Expression of HP1α-GFP or HP1β-GFP in wild-type and HP1α/β-null MEFs yielded, in both cases, distinctly heterochromatic patterns (Fig. 6C, HP1α-gfp and HP1β-gfp), suggesting that these variants have an inherent heterochromatin-targeting ability and that their localization patterns are not inter-dependent. However, this was not the case with HP1γ: when HP1γ-GFP was expressed in wild-type MEFs, the newly made protein was targeted preferentially to heterochromatin (as in other mouse cells), but this was never observed in HP1α/β-null MEFs (Fig. 6C, HP1γ-gfp). Thus, HP1γ does not seem to have an inherent heterochromatin binding ability and can only be recruited to heterochromatic sites via HP1α or HP1β, or an HP1α- or HP1β-associated factor.

Regardless of the differences in localization, 'diffuse' and 'heterochromatin-focused' HP1γ-GFP exhibited similar dynamics in HP1α/β-null and wild-type MEFs (Fig. 6D). By contrast, HP1α-GFP and HP1β-GFP showed a much higher mobility in HP1α/β-null cells (Fig. 6D, see corresponding entries), despite the fact that their overall localization patterns were similar to those seen in wild-type cells.

Discussion

A HP1 'repertoire'?

The work presented here addresses topical questions that have recently emerged in the literature: does HP1 always follow code? (Li et al., 2002); and, is this protein a ubiquitous structural component of heterochromatin? (Hediger and Gasser, 2006). To answer these questions, we have tried to accumulate critical information that would allow us to make the distinction between cell context-related features and 'universal' rules of HP1 organization that are followed in all cells. A similar logic has been adopted in several recent publications, comparing, among other things, the expression of HP1 proteins in mouse and avian erythrocytes (Gilbert et al., 2003), the dynamics of HP1 in undifferentiated and differentiated ES cells (Meshorer et al., 2006) and the genome-wide partitioning of HP1 between euchromatic and heterochromatic loci (de Wit et al., 2007).

Screening ten mammalian lines, undifferentiated and partially differentiated ES cells and wild-type or HP1-null embryonic fibroblasts we have documented the existence of alternative distribution patterns of HP1 proteins. Similar results have been obtained by examining numerous human or mouse tissues in vivo [see companion article by Ritou et al. (Ritou et al., 2007)], strongly suggesting that HP1 organization is rather heterogeneous and largely cell-context dependent.

The existence of this 'plasticity' can be better understood in the light of new observations, which suggest that combinatorial histone modifications occurring near regulated genes exhibit 'pulsing' (Azuara et al., 2006; Gan et al., 2007). This would explain how the various cells of a given microenvironment (e.g. stem cell niche) develop differential responsiveness to extracellular stimuli and why histone modifications and HP1 localization patterns do not match exactly on a single-cell level.

That said, the dynamic transitions of HP1 proteins could be important from a functional perspective. As recently suggested by Misteli (Misteli, 2005), the differential regulation of gene expression might involve the inducible 'potentiation' of genomic loci, with the subsequent displacement from their chromosome territory and translocation to a transcriptionally silencing or activating microenvironment. In this context, the redistribution of HP1 proteins may reflect the dynamic compartmentalization of the cell nucleus under shifting microenvironmental conditions and the continual adaptation of the chromatin network to new metabolic and proliferative regimes. If this were the case, HP1 proteins would be ideal tools for typing cell populations that possess different developmental potential (Fig. 7A).

HP1 dynamics and potential binding states

As explained in the Introduction, recent FRAP studies have unveiled several aspects of HP1 dynamics in mammalian cells (Cheutin et al., 2003; Festenstein et al., 2003; Schmiedeberg et al., 2004; Dialynas et al., 2006). However, an inherent limitation of this approach is that it could only measure average (bulk) properties and not the primary interactions that take place in each chromatin sub-compartment.

The cartoon in Fig. 7B explores what such interactions might involve and represents an attempt to place HP1 dynamics in a realistic, molecular context. A key issue pertinent to HP1 'microstates' is how much of the HP1 protein is 'free' and how much is transiently or stably bound to chromatin at steady-state. Assessing the abundance and distribution of the three HP1 variants after lysis of the cells (at isotonic conditions) with a mild, non-ionic detergent, we have found that a large proportion of the HP1 proteins is washed out of the nucleus, suggesting transient binding to chromatin or no binding at all. Furthermore, comparing HP1 dynamics with HP1 distribution patterns in different cellular contexts, we have noticed that the rate of fluorescence recovery after photobleaching does not always mirror accumulation at heterochromatic foci. To take one characteristic example, HP1γ-GFP residing in heterochromatic blocks (wild-type MEFs and C127 cells) showed almost the same recovery half-times as diffusely distributed HP1γ-GFP (HP1α/β-null MEFs and HeLa cells). Similarly, whereas the fluorescence recovery half-times of HP1α/β-GFP dropped moderately (less than 50%) when the cells were treated with TSA or butyrate, their corresponding localization patterns were markedly different from those seen in untreated cells. Cheutin et al. (Cheutin et al., 2003) have reported the same result, although their interpretation was slightly different. Consequently, the mobility of HP1-GFP proteins (as assessed by FRAP) does not represent, by itself, a distinguishing feature of heterochromatic versus euchromatic association, or a predictive rule that could tell us what proportion of the protein is recruited at heterochromatic foci at a given time.

Of course, the larger issue here is which model should be adopted in order to 'translate' FRAP data into binding states and residence times. Intuitively, the diffuse, pan-chromatic distribution often observed with HP1γ or HP1α makes attractive a '3D genome-scanning' model (Phair et al., 2004; van Holde and Zlatanova, 2006), which explains very well the rapid 'surveying' of potential binding sites across the entire nucleus and is consistent with the occasional weak association with epigenetically marked regions residing either in euchromatin or heterochromatin (with regards to the latter it should be taken into account that the K_ds of HP1 binding to K9-trimethylated histone H3 are at the μM range). However, for situations that might be far from equilibrium or involve diffusion in a restricted volume (e.g. HP1α and HP1γ redistribution in ES cells and stimulated lymphocytes), a more complex reaction-diffusion mechanism (Sprague et al., 2004;

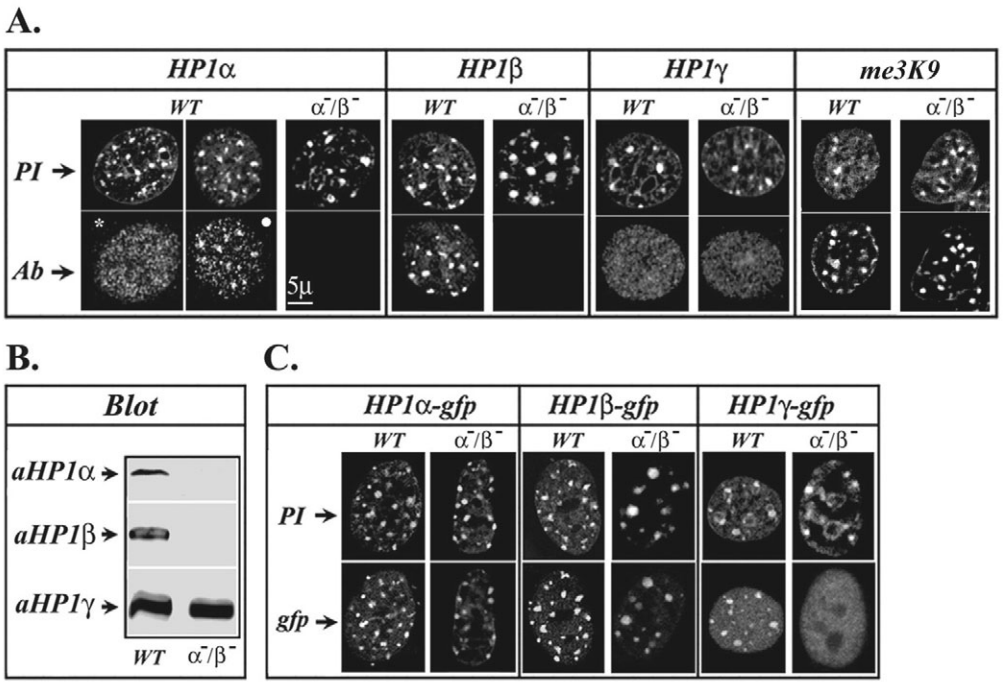

D.

Morphometry		
protein	cell type	speckles per cell
HP1α	WT (SP)	21
HP1α	α⁻/β⁻ (SP)	22
HP1β	WT (SP)	22
HP1β	α⁻/β⁻ (SP)	16
HP1γ	WT (SP)	19
HP1γ	α⁻/β⁻ (D)	0

E.

FRAP					
protein	cell type	im. fr.%	$t_{1/2}$	$r t_{1/2}$	# exp.
HP1α	WT (SP)	5.0	7.0	1.84	10
HP1α	α⁻/β⁻ (SP)	1.3	3.8		10
HP1β	WT (SP)	4.1	10.0	2.56	16
HP1β	α⁻/β⁻ (SP)	2.3	3.9		10
HP1γ	WT (SP)	1.1	3.7	1.37	10
HP1γ	α⁻/β⁻ (D)	1.3	2.7		15

Fig. 6. Distribution and dynamics of HP1 proteins in wild-type and mutant MEFs. (A) Localization of endogenous HP1α, HP1β, HP1γ and me_3K9-histone H3 in wild-type MEFs (WT) and HP1α-HP1β double null mutants (α^-/β^-). Propidium iodide (PI) and antibody staining (Ab) are shown. (B) Western blot on WT and α^-/β^- cells with the three anti-HP1 antibodies. (C) Distribution of HP1-GFP protein variants in the two cell types used above. Propidium iodide (PI) and GFP fluorescence are shown. Notice the different distribution of HP1γ-GFP in WT and α^-/β^- cells. (D) The average number of HP1 foci (2 μm or greater in diameter) in transfected cells. (E) FRAP data from transfected WT and α^-/β^- cells. $rt_{1/2}$ is the ratio of the half-times in the two cell types; im. fr. is the immobile fraction. Bar, 5 μm.

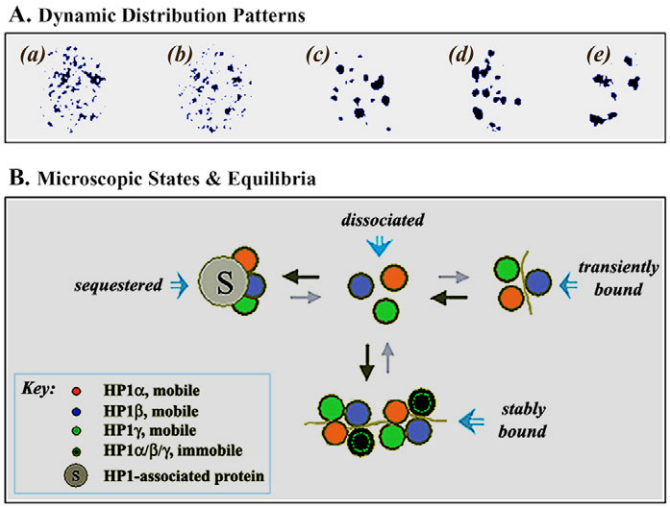

Fig. 7. Hypothetical model explaining HP1 plasticity. (A) Characteristic patterns of HP1 proteins in different cell types and developmental states that could be used as tools for epigenetic cell typing. Images collected in the course of this study have been artistically modified to highlight the variations in HP1 localization. (B) Potential microscopic states and equilibria involving HP1 proteins. The central concept in this model is that HP1 proteins are involved in multiple interactions, including self-association and binding to chaperones or assembly factors (gray circle S). A small fraction of HP1 (black circles with inner green circle) binds stably to chromatin, whereas a greater fraction (red, blue and green circles) associates weakly with chromatin territories through me_3K9-H3 or pre-existing HP1. A sub-population of HP1 molecules 'scan' chromatin in a perpetual fashion, whereas another proportion remain freely diffusible in the nucleoplasm. For more details see Discussion.

Beaudouin et al., 2006) may provide an alternative framework for correlating FRAP data with other observations.

Materials and Methods

Cells, treatments and antibodies

Wild-type and mutant mouse embryonic fibroblasts (MEFs) were isolated from mouse embryos. The production and analysis of the single and double knockout animals will be reported independently. HeLa, MCF-7, C127, 3T3, NRK and MDCK-II cells were cultured according to standard procedures. S-phase blockade was effected by treatment with 5 mM hydroxyurea for 24 hours. Cells were treated with the histone deacetylase (HDAC) inhibitors trichostatin A (TSA, 100 ng/ml), sodium butyrate (NaBu, 10 mM), or curcumin (35 μM) for 24 hours. Six variant-specific anti-HP1 antibodies were employed in this survey. Of these, three rat monoclonals against HP1α, HP1β and HP1γ, respectively, have been exhaustively characterized in a cohort of previous studies (Dialynas et al., 2006; Horsley et al., 1996; Kourmouli et al., 2000; Nielsen et al., 1999) and another three mouse monoclonals (Nielsen et al., 2001), were purchased from Euromedex (Souffelweyersheim, France). Screening of genomic databases confirmed that the epitopes recognized by these antibodies were conserved in at least four mammalian species (*Homo sapiens*, *Mus musculus*, *Rattus norvegicus* and *Canis familiaris*), except for canine HP1γ, which diverged in the carboxyl-terminal region (for relevant information on HP1 sequences see www.ensembl.org). The specificity of the antibodies was also confirmed by western blotting. Two anti-me_3K9-H3 antibodies were utilized: one antibody was originally characterized by Cowell et al. (Cowell et al., 2002) and the other was obtained from Abcam (Cambridge, UK).

Transfection

Plasmid DNA (20 μg) was introduced into cultured cells by electroporation using the ECM630 apparatus (Bio-Rad, Richmond, VA, USA). The day before, cells were split so that they would be at 80-85% confluency on the day of use. They were then trypsinized, adjusted to a density of 1.2×10^6/0.4 ml, introduced into a 4 cm electrode gap cuvette and porated at 260 V, 725 Ω and 850 mF.

Microscopy

For light microscopy, samples were fixed with 1-4% formaldehyde in phosphate-buffered saline, permeabilized with 0.2% Triton X-100 and blocked with 0.5% fish skin gelatin. Staining of DNA (propidium iodide) and probing with the relevant primary and secondary antibodies was performed according to the methods of Maison et al. (Maison et al., 1993). The specimens were examined in a Leica SP confocal microscope at the Light and Video Microscopy Facility of the University of Ioannina.

Morphometric analysis

For morphometric analysis we followed a standard routine. First, individual optical sections (0.3-0.4 μm) were viewed in an enlarged format to examine as closely as possible the location of HP1 foci relative to peripheral, perinucleolar and interstitial heterochromatin. Stacks of such sections were then combined (in a 'projection' mode) and the number of HP1 foci, as well as the fluorescence intensity per unit of nuclear surface, was systematically measured using ImageJ. software, allowing a comparison of differently stained specimens. To account for confluence and ploidy differences, these experiments were repeated multiple times (at least 15), using cell aliquots that were thawed, cultured and analyzed independently.

FRAP

Fluorescence recovery after photobleaching (FRAP) assays were performed on a Leica laser scanning confocal microscope using suitable software and the 488-nm line of an argon laser. HP1α/β/γ-GFP-transfeceted cells were grown on special Petri dishes with coverslips attached and visualized in phenol-free culture medium buffered with Hepes-KOH. FRAP was performed employing a 1 μm spot bleach (either on heterochromatic foci, or an area of the nucleoplasm exhibiting diffuse fluorescence) with a triple bleach pulse of 208 mseconds. Bleaching was initiated after 50 pre-bleach images. Five hundred to 1000 images (256×256 pixels) were collected at a rate of 5 frames/second at low laser power (1.5-5% of the maximun value). Fluorescence recovery was monitored for a minimum of 120 seconds and a maximum of 120 minutes, as needed. As controls we used histone H3-GFP-transfected cells (because this protein is basically 'immobile'), or HP1-GFP-transfected cells treated for 10 minutes with 3% paraformaldehyde (fluorescence recovery completely inhibited by fixation). For normalizing the data, we always corrected for fluorescence quench and recovery observed in the entire cell and in the background.

This project was supported by an EPAN grant to S.D.G. from the Greek Secretariat of Research and Technology and a graduate fellowship to G.K.D. from the Institute of Research and Technology (IBE-ITE). We thank I. Giannios for assistance and D. Makatsori, N. Kourmouli, A. Melidoni and P. Kouklis for valuable suggestions or materials. Morphological work was performed at the Confocal and Video Microscopy Unit of the University of Ioannina.

The paper is dedicated to George Mathianakis.

References

Azuara, V., Perry, P., Sauer, S., Spivakov, M., Jørgensen, H. F., John, R. M., Gouti, M., Casanova, M., Warnes, G., Merkenschlager, M. et al. (2006). Chromatin signatures in pluripotent stem cell lines. *Nat. Cell Biol.* **8**, 532-538.

Bannister, A. J., Zegerman, P., Partridge, J. F., Miska, E. A., Thomas, J. O., Allshire, R. C. and Kouzarides, T. (2001). Selective recognition of methylated lysine 9 on histone H3 by the HP1 chromo domain. *Nature* **410**, 120-124.

Bartova, E., Pachernik, J., Harnicarova, A., Kovarik, A., Kovarikova, M., Hofmanova, J., Skalnikova, M., Kozubek, M. and Kozubek, S. (2005). Nuclear levels and patterns of histone H3 modification and HP1 proteins after inhibition of histone deacetylases. *J. Cell Sci.* **118**, 5035-5046.

Bartova, E., Pachernik, J., Kozubik, A. and Kozubek, S. (2007). Differentiation-specific association of HP1alpha and HP1beta with chromocentres is correlated with clustering of TIF1beta at these sites. *Histochem. Cell Biol.* **127**, 375-388.

Beaudouin, J., More-Bermudez, F., Klee, T., Daigle, N. and Ellenberg, J. (2006). Dissecting the contribution of diffusion and interactions to the mobiity of nuclear proteins. *Biophys. J.* **90**, 1878-1894.

Brasher, S. V., Smith, B. O., Fogh, R. H., Nietlispach, D., Thiru, A., Nielsen, P. R., Broadhurst, R. W., Ball, L. J., Murzina, N. V. and Laue, E. D. (2000). The structure of mouse HP1 suggests a unique mode of single peptide recognition by the shadow chromo domain dimer. *EMBO J.* **19**, 1587-1597.

Cammas, F., Janoshazi, A., Lerouge, T. and Losson, R. (2007). Dynamic and selective interactions of the transcriptional corepressor TIF1beta with the heterochromatin protein HP1 isotypes during cell differentiation. *Differentiation* **75**, 627-637.

Cheutin, T., McNairn, A. J., Jenuwein, T., Gilbert, D. M., Singh, P. B. and Misteli, T. (2003). Maintenance of stable heterochromatin domains by dynamic HP1 binding. *Science* **299**, 721-725.

Cowell, I. G., Aucott, R., Mahadevaiah, S. K., Burgoyne, P. S., Huskisson, N., Bongiorni, S., Prantera, G., Fanti, L., Pimpinelli, S., Wu, R. et al. (2002). Heterochromatin, HP1 and methylation at lysine 9 of histone H3 in animals. *Chromosoma* **111**, 22-36.

Cowieson, N. P., Partridge, J. F., Allshire, R. C. and McLaughlin, P. J. (2000). Dimerisation of a chromo shadow domain and distinctions from the chromodomain as revealed by structural analysis. *Curr. Biol.* **10**, 517-525.

de Wit, E., Greil, F. and van Steensel, B. (2007). High-resolution mapping reveals links of HP1 with active and inactive chromatin components. *PLoS Genet.* **3**, e38.

Dialynas, G. K., Makatsori, D., Kourmouli, N., Theodoropoulos, P. A., McLean, K., Terjung, S., Singh, P. B. and Georgatos, S. D. (2006). Methylation-independent binding to histone H3 and cell cycle-dependent incorporation of HP1beta into heterochromatin. *J. Biol. Chem.* **281**, 14350-14360.

Eissenberg, J. C. and Elgin, S. C. (2000). The HP1 protein family: getting a grip on chromatin. *Curr. Opin. Genet. Dev.* **10**, 204-210.

Eskeland, R., Eberharter, A. and Imhof, A. (2007). HP1 binding to chromatin methylated at H3K9 is enhanced by auxiliary factors. *Mol. Cell. Biol.* **27**, 453-465.

Festenstein, R., Pagakis, S. N., Hiragami, K., Lyon, D., Verreault, A., Sekkali, B. and Kioussis, D. (2003). Modulation of heterochromatin protein 1 dynamics in primary mammalian cells. *Science* **299**, 719-721.

Filesi, I., Cardinale, A., van der Sar, S., Cowell, I. G., Singh, P. B. and Biocca, S. (2002). Loss of heterochromatin protein 1 (HP1) chromodomain function in mammalian cells by intracellular antibodies causes cell death. *J. Cell Sci.* **115**, 1803-1813.

Gan, Q., Yoshida, T., McDonald, O. G. and Owens, G. K. (2007). Epigenetic mechanisms contribute to pluripotency and cell lineage determination of embryonic stem cells. *Stem Cells* **25**, 2-9.

Gilbert, N., Boyle, S., Sutherland, H., de Las Heras, J., Allan, J., Jenuwein. T. and Bickmore, W. A. (2003). Formation of facultative heterochromatin in the absence of HP1. *EMBO J.* **22**, 5540-5550.

Hediger, F. and Gasser, S. M. (2006). Heterochromatin protein 1, don't judge the book by its cover! *Curr. Opin. Genet. Dev.* **16**, 143-150.

Horsley, D., Hutchings, A., Butcher, G. W. and Singh, P. B. (1996). M32, a murine homologue of Drosophila heterochromatin protein 1 (HP1), localises to euchromatin within interphase nuclei and is largely excluded from constitutive heterochromatin. *Cytogenet. Cell Genet.* **73**, 308-311.

Jacobs, S. A. and Khorasanizadeh, S. (2002). Structure of HP1 chromodomain bound to a lysine 9-methylated histone H3 tail. *Science* **295**, 2080-2083.

Jones, D. O., Cowell, I. G. and Singh, P. B. (2000). Mammalian chromodomain proteins: their role in genome organisation and expression. *BioEssays* **22**, 124-137.

Kourmouli, N., Theodoropoulos, P. A., Dialynas, G., Bakou, A., Politou, A. S., Cowell, I. G., Singh, P. B. and Georgatos, S. D. (2000). Dynamic associations of heterochromatin protein 1 with the nuclear envelope. *EMBO J.* **19**, 6558-6568.

Lachner, M., O'Carroll, D., Rea, S., Mechtler, K. and Jenuwein, T. (2001). Methylation of histone H3 lysine 9 creates a binding site for HP1 proteins. *Nature* **410**, 116-120.

Li, Y., Kirschmann, D. A. and Wallrath, L. L. (2002). Does heterochromatin protein 1 always follow code? *Proc. Natl. Acad. Sci. USA* **99**, 16462-16469.

Lomberk, G., Bensi, D., Fernandez-Zapico, M. E. and Urrutia, R. (2006). Evidence for the existence of an HP1-mediated subcode within the histone code. *Nat. Cell Biol.* **8**, 407-415.

Maison, C., Horstmann, H. and Georgatos, S. D. (1993). Regulated docking of nuclear membrane vesicles to vimentin filaments during mitosis. *J. Cell Biol.* **123**, 1491-1505.

Maison, C., Bailly, D., Peters, A. H., Quivy, J. P., Roche, D., Taddei, A., Lachner, M., Jenuwein, T. and Almouzni, G. (2002). Higher-order structure in pericentric heterochromatin involves a distinct pattern of histone modification and an RNA component. *Nat. Genet.* **30**, 329-334.

Meshorer, E., Yellajoshula, D., George, E., Scambler, P. J., Brown, D. T. and Misteli, T. (2006). Hyperdynamic plasticity of chromatin proteins in pluripotent embryonic stem cells. *Dev. Cell* **10**, 105-116.

Minc, E., Allory, Y., Worman, H. J., Courvalin, J. C. and Buendia, B. (1999). Localization and phosphorylation of HP1 proteins during the cell cycle in mammalian cells. *Chromosoma* **108**, 220-234.

Misteli, T. (2005). Concepts in nuclear architecture. *BioEssays* **27**, 477-487.

Nichols, J., Evans, E. P. and Smith, A. G. (1990). Establishment of germ-line-competent embryonic stem (ES) cells using differentiation inhibiting activity. *Development* **110**, 1341-1348.

Nielsen, A. L., Ortiz, J. A., You, J., Oulad-Abdelghani, M., Khechumian, R., Gansmuller, A., Chambon, P. and Losson, R. (1999). Interaction with members of the heterochromatin protein 1 (HP1) family and histone deacetylation are differentially involved in transcriptional silencing by members of the TIF1 family. *EMBO J.* **18**, 6385-6395.

Nielsen, A. L., Oulad-Abdelghani, M., Ortiz, J. A., Remboutsika, E., Chambon, P. and Losson, R. (2001). Heterochromatin formation in mammalian cells: interaction between histones and HP1 proteins. *Mol. Cell* **7**, 729-739.

Phair, R. D., Scaffidi, P., Elbi, C., Vecerova, J., Dey, A., Ozato, K., Brown, D. T., Hager, G., Bustin, M. and Misteli, T. (2004). Global nature of dynamic protein-chromatin interactions in vivo: three-dimensional genome scanning and dynamic interaction networks of chromatin proteins. *Mol. Cell. Biol.* **24**, 6393-6402.

Pinol-Roma, S. (1999). Association of nonribosomal nucleolar proteins in ribonucleoprotein complexes during interphase and mitosis. *Mol. Biol. Cell* **10**, 77-90.

Ritou, E., Bai, M. and Georgatos, S. D. (2007). Variant-specific patterns and humoral regulation of HP1 proteins in human cells and tissues. *J. Cell Sci.* **120**, 3425-3435.

Schmiedeberg, L., Weisshart, K., Diekmann, S., Meyer Zu Hoerste, G. and Hemmerich, P. (2004). High- and low-mobility populations of HP1 in heterochromatin of mammalian cells. *Mol. Biol. Cell* **15**, 2819-2833.

Schott, S., Coustham, V., Simonet, T., Bedet, C. and Palladino, F. (2006). Unique and redundant functions of C. elegans HP1 proteins in post-embryonic development. *Dev. Biol.* **298**, 176-187.

Singh, P. B. and Georgatos, S. D. (2002). HP1: facts, open questions, and speculation. *J. Struct. Biol.* **140**, 10-16.

Singh, P. B., Miller, J. R., Pearce, J., Kothary, R., Burton, R. D., Paro, R., James, T. C. and Gaunt, S. J. (1991). A sequence motif found in a Drosophila heterochromatin protein is conserved in animals and plants. *Nucleic Acids Res.* **19**, 789-794.

Smothers, J. F. and Henikoff, S. (2001). The hinge and chromo shadow domain impart distinct targeting of HP1-like proteins. *Mol. Cell. Biol.* **21**, 2555-2569.

Sprague, B. L., Pego, R. L., Stavreva, D. A. and McNally, J. G. (2004). Analysis of binding reactions by fluorescence recovery after photobleaching. *Biophys. J.* **86**, 3473-3495.

van Holde, K. and Zlatanova, J. (2006). Scanning chromatin: a new paradigm? *J. Biol. Chem.* **281**, 12197-12200.

Zatsepina, O. V., Todorov, I. T., Philipova, R. N., Krachmarov, C. P., Trendelenburg, M. F. and Jordan, E. G. (1997). Cell cycle-dependent translocations of a major nucleolar phosphoprotein, B23, and some characteristics of its variants. *Eur. J. Cell Biol.* **73**, 58-70.